



LAWRENCE
LIVERMORE
NATIONAL
LABORATORY

Architecture, design, and numerical simulation of a code/pulse-position-swapping (CPPS) direct translating receiver

A. J. Mendez, V. J. Hernandez, C. V. Bennett, R. M. Gagliardi

January 19, 2011

SPIE Photonics West
San Francisco, CA, United States
January 22, 2011 through January 27, 2011

Disclaimer

This document was prepared as an account of work sponsored by an agency of the United States government. Neither the United States government nor Lawrence Livermore National Security, LLC, nor any of their employees makes any warranty, expressed or implied, or assumes any legal liability or responsibility for the accuracy, completeness, or usefulness of any information, apparatus, product, or process disclosed, or represents that its use would not infringe privately owned rights. Reference herein to any specific commercial product, process, or service by trade name, trademark, manufacturer, or otherwise does not necessarily constitute or imply its endorsement, recommendation, or favoring by the United States government or Lawrence Livermore National Security, LLC. The views and opinions of authors expressed herein do not necessarily state or reflect those of the United States government or Lawrence Livermore National Security, LLC, and shall not be used for advertising or product endorsement purposes.

Architecture, design, and numerical simulation of a code/pulse-position-swapping (CPPS) direct translating receiver

Antonio J. Mendez^{*a}, Vincent J. Hernandez^b, Corey V. Bennett^b, Robert M. Gagliardi^c

^aMendez R&D Associates (MRDA), PO Box 2756, El Segundo, CA USA 90245-1856;

^bLawrence Livermore National Laboratory (LLNL); Livermore, CA USA 94550;

^cUniversity of Southern California, Department of Electrical Engineering-Systems, Los Angeles, CA USA 90089

ABSTRACT

Code/pulse-position-swapping (CPPS) is a communications scheme that substitutes pulse-position-modulation (PPM) symbols with optical-code-division-access (O-CDMA) codes. CPPS retains the multiple bits per symbol communication of M -ary PPM and the asynchronous multiple access of O-CDMA. Additionally, CPPS has the advantages of granular communications, common electrical bandwidth for all users independent of data rates, compatibility with free-space or guided (fiber and waveguide) communication links, and compatibility with intensity modulation/direct detection. The transmitted symbols (codes) of CPPS are translated from a deserialized bit stream that has been divided into words of length $\log_2 M$. Thus the receivers associate the detected symbol with the original bit sequence by means of an electronically implemented look-up-table (LUT). This paper describes the architecture and design of a direct translating receiver based on map-coding, which uses optical processing to output the transmitted bit sequence without the need for a LUT. Analyses and computations characterize the receiver concept in terms of bit errors (mistranslations).

Keywords: Modulation and coding, pulse-position-modulation (PPM), optical-code-division-multiple-access (O-CDMA), 2D O-CDMA codes, wavelength/time matrix codes, optical communications, planar lightwave circuits (PLCs)

INTRODUCTION

Pulse position modulation (PPM) is recognized as a power efficient means of communication¹ favored for communication links that are average power limited (such as space links). The advantages of PPM can be combined with multiple access communications by substituting the pulse positions with optical-code-division-multiple-access (O-CDMA) codes²⁻⁵. This technique is known as code/pulse-position-swapping (CPPS). CPPS retains the multiple bits per symbol communication of PPM as well as the asynchronous multiple access of O-CDMA. Additionally, CPPS allows variable data rates or bits per symbol for each user (granular communications); common electrical bandwidth for all users at all data rates; network reconfigurability; compatibility with free-space or guided (fiber and waveguide) communication links; and compatibility with intensity modulation/direct detection, depending on the selection of the O-CDMA codes. Table I depicts the granular communications and reconfigurability for the case of 32 pseudo-orthogonal codes. It shows that various combinations of M -ary CPPS transmissions yield different peak bits/symbol, data rates, throughput, and quality-of-service (QoS).

PPM and CPPS transmission involves taking a serial bit stream and segmenting it or demultiplexing it into sets or words of length $\log_2 M$. Usually, a computer converts these words into symbols, but optical processing through a switch and delay line array can also perform the conversion for higher data rates and large values of M ⁶. On the receiver side, a decision test identifies the transmitted symbol, typically by comparing the symbol space (either pulse positions or codes) and determining which contains the most power. After this decision, a look-up-table (LUT) translates the symbol back to its original binary word. Again, electronic processing typically performs the comparison test and LUT; however, this becomes impractical when the combination of high data rates and/or large M leads to very short decision times. For these cases, we have been exploring receiver architectures for both PPM and CPPS that perform the decision test while simultaneously directly declaring (translating) the initial bit set through optical processing.

^{*}MendezRDA@AOL.com; phone 1 310 640-0497; fax 1 310 640-1774

This paper describes the architecture and design of direct translating receivers for CPPS, which we designate as correlating receivers (CR). Based on map coding, these CRs improve upon a previously proposed CPPS receiver² that did not have direct translating capability but required a bank of correlators for each user and multiuser detection⁷. The CRs described use a known set of 32 wavelength/time codes⁸, and as shown in Table I, can potentially support the M -ary cases of 32, 16, 8, 4, and 2.

The performance of CPPS and the CR is explored by focusing on the highlighted row in Table I ($M=16,8,4,4$). We describe the architecture of the network and the CR, the design of the CR, and the performance of CPPS in terms of bit declarations by the CR. The CR design is based on planar lightwave circuits (PLCs) with lossless splitting (by virtue of erbium doped waveguide amplifiers, EDWAs), delay lines, and differential photodetectors that affect signal polarity.

Table 1. Potential Granular Communications Combinations Based on CPPS for the Case of 32 Codes.

Concurrent Users	Codes/User	Bits/Symbol (Code)	Relative Throughput	Highest Bits/Frame Time	QoS
1	32	5	5	5	Very High
2	16,16	4,4	8	4	Very High
4	8,8,8,8	3,3,3,3	12	3	High
4	16,8,4,4	4,3,2,2	11	4	High
5	8,8,8,4,4	3,3,3,2,2	13	3	High
6	8,8,4,4,4,4	3,3,2,2,2,2	14	3	High
7	8,4,4,4,4,4,4	3,2,2,2,2,2,2	15	3	High
7	8,8,8,2,2,2,2	3,3,3,1,1,1,1	13	3	Moderate
8	8,4,4,4,4,4,2,2	3,2,2,2,2,2,1,1	15	3	Moderate
10	8,4,4,4,2,2,2,2,2,2	3,2,2,2,1,....1	15	3	Moderate
16	2,2,2,.....2	1,1,.....1	16	1	Fair

TECHNICAL DISCUSSION

2.1 Scope

The following subsections describe: the network architecture associated with the highlighted row of Table I, the generalized implementation of direct translating receivers and the notion of map coding, the architecture (design guidelines) of a CR based on map coding, and the actual design of a CR. Analyses and computations then illustrate the performance of the CR in the single user and multiuser cases.

2.2 Network architecture

Figure 1 shows the CPPS network architecture. Since we use wavelength/time (W/T) matrix codes (MC), the system can be based on an encodable carrier consisting of pulse trains whose repetition rate corresponds to the frame rate. The pulses contain all wavelengths in the code set. The carrier broadcasts to all users, and the users locally construct a code representative of the symbol to be transmitted. As shown in Figure 1, User 1 is assigned the first sixteen codes, User 2 the next eight, User 3 the next four, and User 4 the last four. The users broadcast their particular code across a shared media (free space or fiber), and CR_i recovers the code transmitted by User i . CR_i translates the received symbol into its equivalent binary word of length $N = \log_2 M$, composed of bits b_{ij} where $0 \leq j < N$. Multiple access interference from the other users may affect this final outcome.

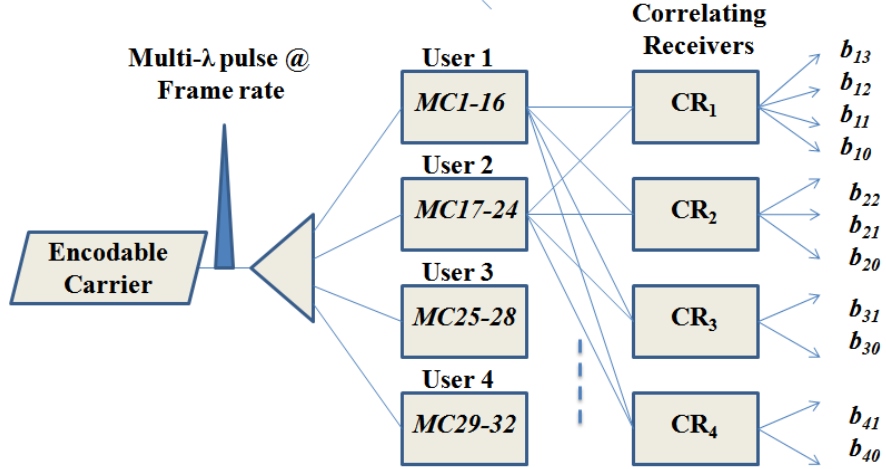


Figure 1. CPPS network architecture for the granular communications case highlighted in Table I, based on matrix codes $MC1$ - $MC32$.

The users construct their codes using the design shown in Figure 2. Since many of the W/T codes are complementary, a single arrayed waveguide grating (AWG) can construct two complementary codes in conjunction with suitable delay line arrays and couplers.

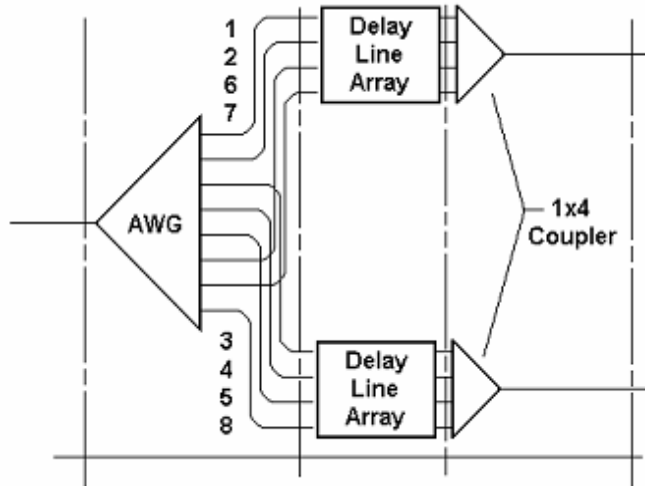


Figure 2. Construction of complementary codes based on one AWG, delay line arrays defining the MCs, and combiners (couplers), demonstrated for codes $MC17$ (wavelengths 1,2,6,7) and $MC13$ (wavelengths 3,4,5,8).

2.3 Direct Translating Receivers and Map coding

Direct translating receivers, whether PPM- or CPPS-based, utilize linear optical processing to identify transmitted symbols and translate them to their equivalent binary word. Similar to their electronic equivalents, they identify symbols through a comparison test between the symbol space (pulse positions or codes), where the space containing the most optical power indicates the transmitted symbol. In its simplest (or generalized) form, this is done by making M copies of an incoming symbol (using couplers) and sending each copy through a symbol processor. The processor then evaluates the symbol against one of the possible symbol spaces. For the PPM case, the symbol processor composes of a simple delay line that aligns the received pulse against a slot. At the sampling time, the processor either outputs the received pulse (when the pulse aligns to the pulse position) or nothing/noise (when the pulse is misaligned with the pulse position). For CPPS, the symbol processors consist of optical decoders of similar structure to Figure 2, outputting either a pulse autocorrelation (for correct decoding) or multiple access interference (for incorrect decoding). At this point, one could conceivably attach individual photodetectors to each symbol processor and compare the photodetector outputs, and a LUT could subsequently translate the photodetector signals into binary. The direct translating receiver improves upon this by performing the LUT translation optically. The output of each symbol processor is optically coupled to yield $N=\log_2 M$ copies, where each copy represents a bit of the binary word. Differential detectors then impart the value of the bit onto the copy. A copy sent into the positive port of the differential detector yields a bit value of 1 when the receiver threshold is set to zero, and a copy sent into the negative port yields a bit value of 0. This translation is made more efficient by optically combining copies from multiple symbol processors into a single port, such that only a single differential photodetector is required for each bit.

The exact assignment of the copies to the positive or negative ports of the differential photodetectors is prescribed through a graphical algorithm called map coding. We apply map coding for the CPPS case to assist us in defining the CR, and Figures 3-5 demonstrate the various highlighted cases of Table I. N tables are created listing the outputs of the decoders, identified by their MC. Each table is then assigned to a photodetector yielding bit b_{ij} . The MCs within each table are partitioned into $2^{*(N-j)}$ sets, and every other set (starting with the first set) is colored. The colored MCs thus designate that the decoder output is to be routed to the negative port, while uncolored entries designate routing to the positive port. Mathematically, this routing can be interpreted respectively as a multiplication of the code by -1 or +1. The differential photodetector output is thus the sum of the positive MCs subtracted by the sum of the negative MCs, with a positive outcome representing a bit value of $b_{ij}=1$ and a zero or negative outcome representing a bit value of $b_{ij}=0$. This mathematical equivalent is expressed underneath each table in Figures 3-5. Note that the map coding can also be interpreted as a simple LUT, with colored codes interpreted as $b_{ij}=0$, and uncolored codes as $b_{ij}=1$.

MC1	MC2	MC3	MC4	MC5	MC6	MC7	MC8
MC9	MC10	MC11	MC12	MC13	MC14	MC15	MC16
$b_{13} = (MC9+MC10+MC11+MC12+MC13+MC14+MC15+MC16)$ $- (MC1+MC2+MC3+MC4+MC5+MC6+MC7+MC8)$							

MC1	MC2	MC3	MC4	MC5	MC6	MC7	MC8
MC9	MC10	MC11	MC12	MC13	MC14	MC15	MC16
$b_{12} = (MC5+MC6+MC7+MC8+MC13+MC14+MC15+MC16)$ $- (MC1+MC2+MC3+MC4+MC9+MC10+MC11+MC12)$							

MC1	MC2	MC3	MC4	MC5	MC6	MC7	MC8
MC9	MC10	MC11	MC12	MC13	MC14	MC15	MC16
$b_{11} = (MC3+MC4+MC7+MC8+MC11+MC12+MC15+MC16)$ $- (MC1+MC2+MC5+MC6+MC9+MC10+MC13+MC14)$							

MC1	MC2	MC3	MC4	MC5	MC6	MC7	MC8
MC9	MC10	MC11	MC12	MC13	MC14	MC15	MC16
$b_{10} = (MC2+MC4+MC6+MC8+MC10+MC12+MC14+MC16)$ $- (MC1+MC3+MC5+MC7+MC9+MC11+MC13+MC15)$							

Figure 3. Map coding for User 1 and $M=16$.

MC17	MC18	MC19	MC20	MC21	MC22	MC23	MC24
------	------	------	------	------	------	------	------

$$b_{22} = (MC21+MC22+MC23+MC24) - (MC17+MC18+MC19+MC20)$$

MC17	MC18	MC19	MC20	MC21	MC22	MC23	MC24
------	------	------	------	------	------	------	------

$$b_{21} = (MC19+MC20+MC23+MC24) - (MC17+MC18+MC21+MC22)$$

MC17	MC18	MC19	MC20	MC21	MC22	MC23	MC24
------	------	------	------	------	------	------	------

$$b_{20} = (MC18+MC20+MC22+MC24) - (MC17+MC19+MC21+MC23)$$

Figure 4. Map coding for User 2 and $M=8$.

MC25	MC26	MC27	MC28
------	------	------	------

$$b_{31} = (MC27+MC28) - (MC25+MC26)$$

MC25	MC26	MC27	MC28
------	------	------	------

$$b_{30} = (MC26+MC28) - (MC25+MC27)$$

MC29	MC30	MC31	MC32
------	------	------	------

$$b_{41} = (MC31+MC32) - (MC29+MC30)$$

MC29	MC30	MC31	MC32
------	------	------	------

$$b_{40} = (MC30+MC32) - (MC29+MC31)$$

Figure 5. Map coding for Users 3 and 4 with $M=4$.

2.4 Architecture of the correlating receiver

The map coding above can be further used to define the architectures of the CRs. Since the W/T codes used in this study are presented as arrays $MC1-MC32$ ⁸, the mathematical equivalent of the map coding (as expressed in Figures 3-5) can be applied to the codes on an element-by-element basis to produce the composite arrays expressed as CR_{ij} in Figures 6-9. The interpretation of these arrays is similar to the original unmodified MCs. In the original MC, the rows of the array represent the wavelengths of the codes while the columns represent the codes' time slots. Each element in the array has an entry of 1 or 0, with 1 indicating the presence of a pulse for that particular wavelength and time slot, and 0 if that element is vacant. The decoding process thus applies the inverse time slot delays to the pulses, effectively aligning them to a single slot. All pulses are then combined to a single photodetector to form a single autocorrelation pulse when the correct code is received.

For the unmodified MCs, the decoder architecture is implicit in the array representation. A similar architecture for the modules of a CR can be derived from the composite array CR_{ij} , except multiple MCs are now being interpreted simultaneously to produce a final bit output of b_{ij} . The row and columns of any non-zero element respectively indicate the wavelength and time slot positioning of received codes, dictating the inverse delays required to realign the code pulses. Elements with absolute values exceeding one (weight > 1) indicate the need for duplicated inverse delays. The bit translation of the codes is now incorporated in the polarity of the values, indicating whether the wavelengths (after

alignment) are routed to the positive or negative ports of the differential receiver. Overall, a complete CR requires N modules, one for each bit of the word. The resulting CR structure is dramatically simplified compared to the generalized description of direct translating receivers, which required M symbol processors. For the CPPS case, this implied that every CR would require M decoders. The modules effectively consolidate the decoders into a single processing unit, greatly reduces the number of optical components required in implementation.

$CR_{13} =$	$CR_{12} =$	$CR_{11} =$	$CR_{10} =$
0	-2	-2	-2
0	0	-2	0
0	0	0	0
0	-2	2	2
-1	0	-1	-2
-1	-1	1	0
-1	1	-1	1
1	1	-1	1
1	-1	1	-1
1	1	1	1
1	1	-1	1
1	1	0	-1
1	3	3	1
-1	1	1	1

Figure 6. CR_{1j} describing the architectures for the CR modules of User 1

$CR_{22} =$	$CR_{21} =$	$CR_{20} =$
-1	-1	-1
0	-1	1
0	1	-1
-1	1	1
-1	1	1
1	-1	1
1	1	0
1	0	0
1	0	0
1	0	0
1	0	0
1	0	0
1	0	0
1	0	0

Figure 7. CR_{2j} for User 2.

$CR_{31} =$	$CR_{30} =$
-1	-1
0	0
0	1
0	0
0	-2
0	0
0	0
0	0
0	0
0	0
0	0
0	0
0	0
0	0

Figure 8. CR_{3j} for User 3.

$CR_{41} =$	$CR_{40} =$
0	0
-1	-1
0	0
0	0
0	0
0	0
0	0
0	0
0	0
0	0
0	0
0	0
0	0
0	0

Figure 9. CR_{4j} for User 4

2.5 Design concept of the correlating receiver

We can now design a CR using the architectures defined above, and have applied it in Figure 10 for CR3. CR3 receives the transmitted signal and decomposes it into its constituent wavelengths by means of an AWG. Each wavelength is then copied by means of a splitter. The number of copies (splitting ratio) equals the maximum number attained by row summing the absolute values of the complete composite array set $\{CR_{ij}\}$, $0 \leq j < N$. For $\{CR_{31} CR_{30}\}$, summing the absolute values of the set across the rows yields 4 for every row except the 6th and 7th rows; therefore 1x4 splitters are used in Figure 10. The splitting ratio performed across each wavelength must be equal (even if this yields unnecessary copies) in order to maintain equal weighting (optical power) for each copy. In these cases, the unused replicas can be used for diagnostic functions. Each wavelength copy becomes representative of a single-weight row element in $\{CR_{ij}\}$. Delay line arrays realign each copy inverse to their element column positioning in CR_{ij} . The copies are then routed to the positive or negative ports of a differential receiver, as prescribed by the element's polarity. Optical couplers precede each port to combine multiple copies, and the actual routing is performed by a function called the interconnect manifold. To overcome insertion losses induced by the splitting losses and interconnections, the design must be based on planar lightwave circuit (PLC) lossless splitters that incorporate erbium doped waveguide amplifiers (EDWAs). The electrical outputs of the differential receivers yield the unthresholded value of b_{ij} .

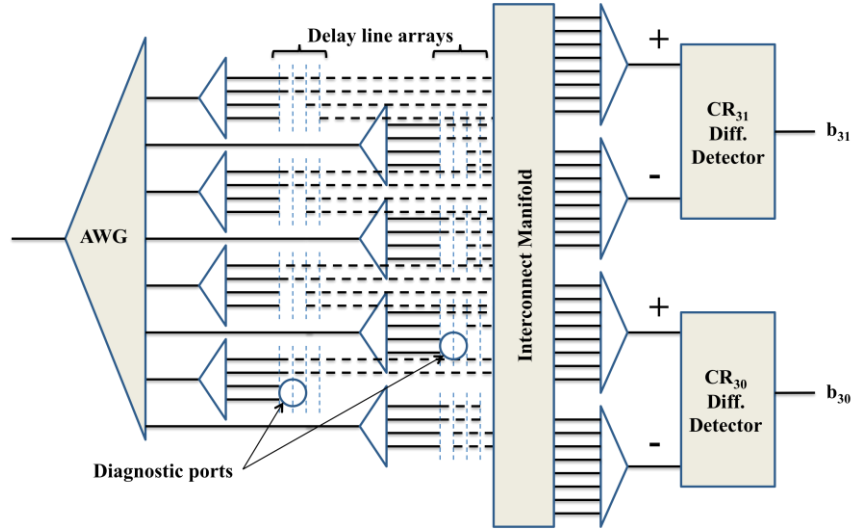


Figure 10. Design of CR3.

2.6 Performance based on simulations

We evaluate the performance of the CR by modeling the case shown in Figure 11 for single user and multiuser operation. In single user operation, User 1 transmits code *MC9* (representing bit sequence *0001*) while the other users remain silent. This measures the performance of CPPS the “PPM mode,” that is, with the time slot only replaced by a code. In multiuser operation, User 1 transmits *MC9* while Users 2,3, and 4 respectively transmit codes *MC19*, *MC26*, and *MC29*. This assesses the effect of multiuser interference on the CR, as generated from the other users. In order to model a worst-case scenario, all users transmit simultaneously, since this is known to produce the most multiuser interference⁹.

The computations consist of convolving the launched code against each array of $\{CR_{ij}\}$, and are shown in Figures 12 and 13. The centers of the convolutions are sampled, with the sampling window equal in width to the coding time slot, or “chip time.” The sampled outputs represent the differential photodetector outputs b_{ij} prior to thresholding. Figure 12 shows the single user operation, while Figure 13 shows the multiuser operation. In both cases, the normalized outputs aligned with the sampling window correctly recover the bit sequence *0001*, the bit translation of *MC9*. This is especially of note in the multiuser case, as the CR is able to overcome the influence of multiuser interference.

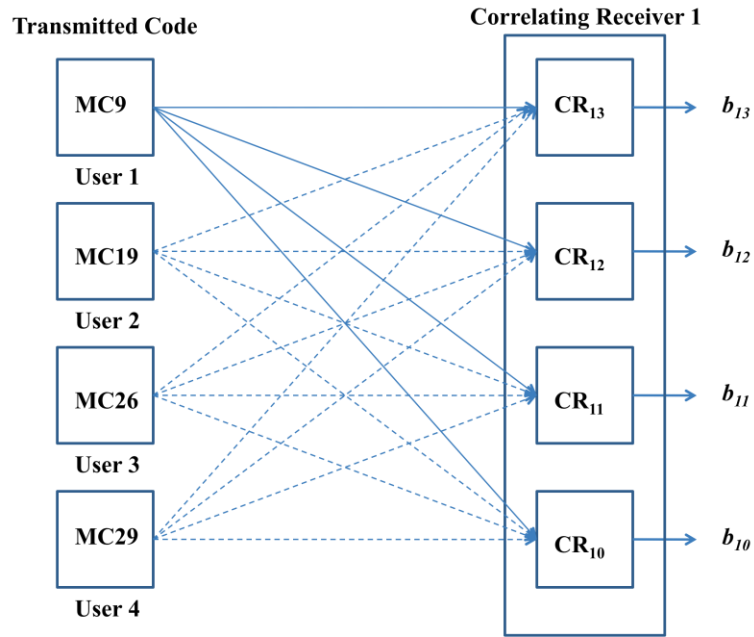


Figure 11. Test case modeled to determine CPPS performance and effect of multiuser interference

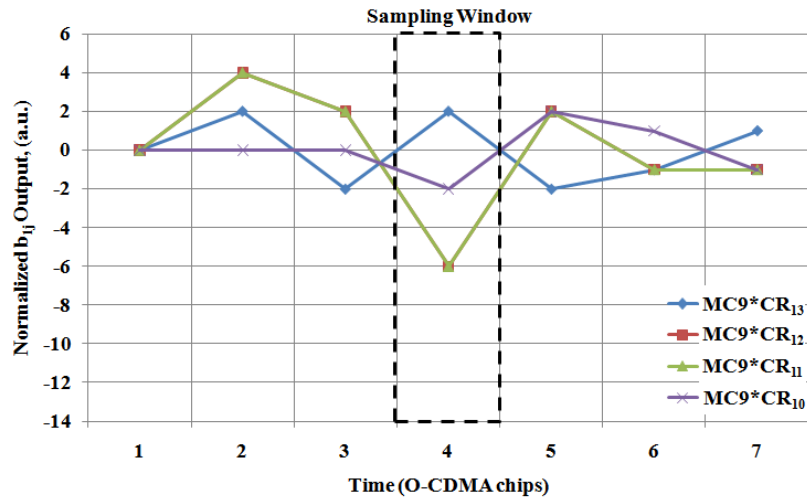


Figure 12. Output of CR1 showing the correlation of a single transmitted code ($MC9$) with individual CR modules (CR_{ij})

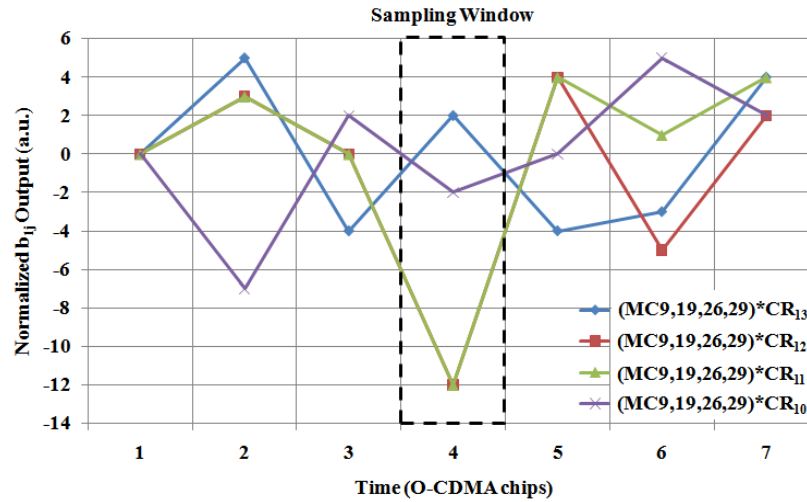


Figure 13. Output of CR1 showing the correlation of transmitted code ($MC9$) with individual CR modules (CR_{ij}) in the presence of multi user interference from codes $MC19, MC26$, and $MC29$.

CONCLUDING REMARKS

This paper has investigated direct translating receivers for CPPS, designated as CRs. The CRs utilize map coding to designate the translation of symbols into their binary equivalent, and the map coding is applied to W/T codes to derive an architecture for designing the CRs. The design incorporates a cascade of optical couplers, and thus requires implementation with PLCs that incorporate EDWAs. Analyses and computations estimated the direct translating function of the CR in the single user and multiuser operation, correctly translating the transmitted symbol in both cases. The analysis did not account for the effect of insertion losses; however, the analysis did assume multiuser synchronous transmission of the signals to yield the maximum multiple access interference. Based on this analysis, we expect that CPPS can be robust and merits further research.

REFERENCES

- [1] R. M. Gagliardi and S. Karp, *Optical Communications*, 2nd ed. New York: John Wiley and Sons, 1995.
- [2] A. J. Mendez, V. J. Hernandez, R. M. Gagliardi, C. V. Bennett, "Code/Pulse Position Swapping (C/PPS) for Multiple-Bits/Symbol and Reconfigurable Multiple Access Communications", IEEE/LEOS Summer Topical Meeting on Optical Code Division Multiple Access, paper TuA4.1, July 2009.
- [3] E. Narimanov, in *Optical Code Division Multiple Access: fundamentals and applications*, P. R. Prucnal, Ed. Boca Raton, FL.: CRC Taylor & Francis, 2006, pp. 106.
- [4] S. Galli, R. Menendez, E. Narimanov, and P. R. Prucnal. "A Novel Method for Increasing the Spectral efficiency of Optical CDMA", IEEE Trans. Comm., vol. 36, no. 12, pp. 2133-2144, 2008.
- [5] X. Wang, N. Wada, T. Miyazaki, G. Cincotti, and K-I. Kitayama, "Asynchronous Multiuser Coherent OCDMA System with Code-Shift-Keying and Balanced Detection", IEEE Selected Topics in Quant. Electronics., vol. 13, no. 5, pp. 1463-1470, 2007.
- [6] A. J. Mendez, V. J. Hernandez, R. M. Gagliardi, and C. V. Bennett, "Transmitter and translating receiver design for 64-ary pulse position modulation (PPM)," in *Proc. SPIE*, vol. 7587, 2010, pp. 75870M-1-7.
- [7] S. Verdú, *Multiuser Detection*, Cambridge University Press, 1998.
- [8] A. J. Mendez, R. M. Gagliardi, V. J. Hernandez, C. V. Bennett, and W. J. Lennon, "High-performance optical CDMA system based on 2-D optical orthogonal codes," *J. Lightw. Technol.*, vol. 22, no. 11, pp. 2409-19, 2004.

- [9] V. J. Hernandez, A. J. Mendez, C. V. Bennett, R. M. Gagliardi, and W. J. Lennon, "Bit-error-rate analysis of a 16-user gigabit ethernet optical-CDMA (O-CDMA) technology demonstrator using wavelength/time codes," *IEEE Photon. Technol. Lett.*, vol. 17, no. 12, pp. 2784-6, Dec. 2005.

ACKNOWLEDGEMENTS

This work performed under the auspices of the U.S. Department of Energy by Lawrence Livermore National Laboratory under Contract DE-AC52-07NA27344. Portions of the work were carried out under a Mendez R&D Associates Independent Research and Development (IR&D) Project. LLNL-CONF-466412